Removal of Arsenic by Bead Cellulose Loaded With Iron Oxyhydroxide From Groundwater

ARTICLE *in* ENVIRONMENTAL SCIENCE AND TECHNOLOGY · OCTOBER 2005

Impact Factor: 5.33 · DOI: 10.1021/es048080k · Source: PubMed

2 AUTHORS, INCLUDING:

Xuejun Guo
Beijing Normal University
26 PUBLICATIONS **528** CITATIONS

SEE PROFILE

Removal of Arsenic by Bead Cellulose Loaded with Iron Oxyhydroxide from Groundwater

XUEJUN GUO* AND FUHUA CHEN
College of Environmental Science and Engineering, Nankai University, Tianjin, China 300071

A new adsorbent, bead cellulose loaded with iron oxyhydroxide (BCF), was prepared and applied for the adsorption and removal of arsenate and arsenite from aqueous systems. The continuing loading process of Fe in the cellulose beads was realized through hydrolization of ferric salts when alkaline solution was added dropwise. Spherical BCF had excellent mechanical and hydraulic properties. Akaganéite (β-FeOOH), the reactive center of BCF that was stably loaded into the cellulose, had a high sensitivity to arsenite as well as arsenate. The maximum content of Fe in BCF reached 50% (w/w). In this study we investigated the adsorption behavior of arsenite and arsenate on BCF, including adsorption isotherms, adsorption kinetics, the influence of pH and competing anions on adsorption, and column experiments. The adsorption data accorded with both *Freundlich* and *Langmuir* isotherms. The adsorption capacity for arsenite and arsenate was 99.6 and 33.2 mg/g BCF at pH 7.0 with an Fe content of 220 mg/mL. Kinetic data fitted well to the pseudo-second-order reaction model. Arsenate elimination was favored at acidic pH, whereas the adsorption of arsenite by BCF was found to be effective in a wide pH range of 5−11. Under the experimental conditions, the addition of sulfate had no effect on arsenic adsorption, whereas phosphate greatly influenced the elimination of both arsenite and aresenate. Silicate moderately decreased the adsorption of arsenite, but not arsenate. Both batch experiments and column experiments indicated that BCF had higher removal efficiency for arsenite than for arsenate. While the influent contaminant concentration was 500 μg/L in groundwater and the empty-bed contact time (EBCT) for arsenite and arsenate was 4.2 and 5.9 min, breakthrough empty-bed volumes at the WHO provisional guideline value of 10 μg/L were 2200 and 5000, respectively. BCF can be effectively regenerated when elution is done with 2 M NaOH solution. The column experiments for four cycles showed that stable and high removal efficiency of arsenic was sustained by BCF after regeneration.

Introduction

Arsenic is classified as one of the most toxic and carcinogenic chemical elements and has been recorded by the World Health Organization as a first priority issue (*1*, *2*). Acute and chronic arsenic exposure via drinking water has been reported in many countries, especially Argentina, Bangladesh, India, Mexico, Mongolia, Thailand, and Taiwan, where a large proportion of groundwater is contaminated with arsenic at levels from 100 to over 2000 μg/L (*3*). Long-term exposure to arsenic in drinking water can lead to cancer of the bladder, lungs, skin, kidney, nasal passages, liver, and prostate. Noncancer effects of ingesting arsenic include cardiovascular, pulmonary, immunological, neurological, and endocrine (e.g., diabetes) disorders (*4*). Besides its tumorigenic potential, arsenic has been shown to be genotoxic (*5*). The United States Environmental Protection Agency (USEPA) has recently lowered the drinking water limit for arsenic to 10 μg/L with a compliance deadline of January 2006 (*6*).

Various treatment technologies have been used to remove arsenic from water. The common methods adopted include (i) coprecipitation (using $Fe_2(SO_4)_3$ or $FeCl_3$) or coagulation with ferric or aluminum salts such as $Al_2(SO_4)\cdot 18H_2O$ as coagulants) (*7*, *8*), (ii) ion exchange (*9*), (iii) use of adsorption media (*10*−*21*), (iv) use of zerovalent iron (*22*, *23*), and (v) reverse osmosis and electrodialysis (*24*).

Among the possible treatment processes, adsorption is considered to be less expensive than membrane filtration, easier and safer to handle as compared to the contaminated sludge produced by precipitation, and more versatile than ion exchange (*6*). The adsorption of arsenic, both as As(III) and as total arsenic, has also been studied using a variety of natural solids, including sand (*17*, *25*), zeolite (*26*), clay mineral (*15*), manganese dioxide (*27*, *28*), and red mud (*29*). The removal of As(III) and As(V) has been studied in detail using activated carbon (*11*) and activated alumina (*10*), as well as lanthanum and zirconium compounds (*30*, *31*), iron hydroxides and oxides (*12*, *13*, *32*, *33*), open-celled cellulose sponge (*14*), and biomass materials (*34*, *35*). To improve arsenic adsorption capacity and selectivity, many adsorbents were prepared by modifying various carriers and media (e.g., sand, resin, zeolite, silica, and activated carbon) with iron and other metal reactive centers (*17*, *21*, *22*, *36*−*40*).

Activated alumina, which is selective in removing As(V), results in 5−10% loss of adsorptive capacity for each run after regeneration (*41*). Polymeric anion exchangers prefer sulfate to arsenate. The arsenic removal capacity is, therefore, greatly reduced in the presence of high concentrations of competing sulfate ions (*42*). Natural solids have broad resources and a low cost, but their arsenic adsorption capacity is often limited unless modified (*43*). Pure iron hydroxides including ferrihydrite, goethite, akaganéite, and lepidocrocite have high affinity toward arsenic, but they usually appear as fine powders, which cannot be applied in fixed-bed columns unless they are of a granular shape (*12*, *16*). Driehaus and co-workers recently developed pressurized granular ferric hydroxide material and tested it for high As(V) removal in fixed beds (*13*). The mechanical strengths and attrition resistance properties of these granular particles are much weaker compared to macromolecule beads (*13*). Selecting a variety of carriers including sands, activated carbon, zeolite, polystyrene, polyHIPE, and carriers loaded with Fe, is the major direction in the preparation of adsorbents applied for the removal of arsenic. But part of the Fe loaded in these carriers always shelled off after long-term use and regeneration. The maximum proportion of Fe loaded reached only 0.1−5% for sands, activated carbon, and zeolite and 7−12% even for macroporous polymers such as polystyrene and polyHIPE (*17*, *21*, *22*, *36*−*40*). Arsenic-contaminated groundwater generally contains both As(III) and As(V) dissolved species in varying proportions (*44*, *45*). Most of the above adsorbents are not effective for As(III) removal unless As(III) has been preoxidized by chlorine, manganese dioxide, ozone,

* Corresponding author phone: +86-22-23503722; fax: +86-22-23508807; e-mail: guoxj21@yahoo.com.cn.

or other innocuous oxidizing agents (*46*−*48*). An ideal adsorbent applied for arsenic removal should have uniformly accessible pores, a high surface area (i.e., high density of adsorption sites), a bead shape, physical and chemical stability, and high affinity for both arsenate and arsenite (*49*).

Cellulose beads are considered to be a promising adsorbent due to their special properties: hydrophilic, porous, high surface area. Cellulose beads and cellulose derivative beads are widely used as ion exchangers, packing materials for chromatography, adsorbents for heavy metal ions and proteins, cosmetic additives, and carriers for immobilization of biocatalysts (*50*−*52*). However, studies on applying cellulose beads as carriers for arsenic removal are still scarce. In this study, we prepared bead cellulose adsorbent loaded with iron oxyhydroxide (BCF) using an innovative and simple method and successfully applied it to the removal of arsenic from groundwater.

Materials and Methods

Chemicals. All chemicals were reagent grade. All glassware was cleaned by being soaked in 15% HNO_3 and rinsed with deionized water.

Preparation of BCF. (1) Preparation of Bead Cellulose. A 16 g portion of degreased cotton was immersed in 400 mL of 20% (m/v) sodium hydroxide for 2−3 h and squeezed to about 75 g. The alkalized cotton was air-proofed and aged for 2−3 days at room temperature. The aged cotton and 8 mL of carbon bisulfide were sealed and shaken at 150 rpm for 4−6 h at room temperature. Then the esterified cellulose was obtained and appeared salmon pink in color. The viscose was prepared by dissolving the esterified cellulose in 6% NaOH solutions and stirring for 3 h. A 500 mL flask equipped with a paddle agitator was filled with 200 mL of chloroben-pump oil (1:2 v/v). Potassium oleate was dissolved in viscose up to 0.2%. At 200−250 rpm, 50 mL of the viscose solution was dispersed in chloroben-pump oil. The reaction flask was heated to 90 °C within 30 min and kept at this temperature for 2 h under continuous stirring. The colored cellulose beads obtained from the reaction flask were filtered and immediately eluted with boiling water until its color changed to snow white. Cellulose beads were stored in deionized water. The 20−60 mesh fraction accounted for 90% (v/v).

(2) Impregnation of Iron. A 100 mL portion of 10% ferric chloride solution ($FeCl_3{\cdot}6H_2O$) and 50 mL of wet bead cellulose were mixed in a 500 mL flask, and then 105 mL of 1 mol/L sodium hydroxide was slowly dropped into the flask at a rate of 10 mL/h under continuous stirring at 200 rpm at room temperature. Along with the addition of alkaline solution, the pH of the supernatant rose and Fe was loaded into the cellulose bead continuously in the form of akaganéite. The residual Fe precipitated when the pH rose to 3.5−4.0 and was eluted out with deionized water three times. The loading processes were repeated seven times, and with an increase of loading times, the Fe content in the cellulose bead increased to 220 ± 20 mg/(mL of beads). The BCF was added with 100 mL of 0.5 mol/L NaOH, shaken for 4 h, and then washed with deionized water several times. The product was stored in deionized water at room temperature for later use (Patent Application Number 200410019876.7, CN).

Arsenic Adsorption Isotherm Tests. Sodium arsenate ($Na_2HAsO_4{\cdot}H_2O$; AR) and arsenic oxide (As_2O_3; AR) were used as arsenic sources. A stock solution of arsenic was prepared at a concentration of 100 mmol/L (pH 7.0) in deionized water. To a series of 250 mL conical flasks were added 50 mL of 1−100 mmol/L arsenic solutions and 1 mL of BCF. The pH was adjusted to 7.0 using 0.1 mol/L HCl or NaOH solutions. All samples were shaken at 150 rpm and 25 ± 0.5 °C in a to-and-fro shaker for 24 h. In the process the pH was readjusted several times to maintain it at 7.0 ± 0.1. After that BCF covered with arsenic was collected. The data of arsenic adsorption were fitted with *Freundlich* and *Langmuir isotherm* models. The Langmuir isotherm is expressed as follows:

$$q_{eq} = \frac{bQ_{max}C_{eq}}{1 + bC_{eq}} \tag{1}$$

where Q_{max} (mg/mL) is the maximum adsorption capacity, C_{eq} (mmol/L) is the equilibrium solute concentration, and b is the equilibrium constant related to the energy of sorption (L/mmol). The Freundlich isotherm is expressed as follows:

$$q_{eq} = KC_{eq}^{\ 1/n} \tag{2}$$

where K is the empirical constant ((mg/mL)/(mmol/L)$^{1/n}$) and n the empirical constant (dimensionless). A nonlinear regression (Microcal Origin 6.0 or 7.0) was applied to obtain all Langmuir and Freundlich isotherm parameters.

Arsenic Adsorption Kinetics. Arsenic stock solution was prepared following the same procedure as described for the adsorption isotherm tests. In a 500 mL flask, 250 mL of arsenic solution and 1 mL of BCF were mixed. The initial arsenic concentration was 7.5 mg/L. The suspension was stirred at 200 rpm. The initial pH of the solution was 7.0, and the temperature was kept at 25 ± 0.5 °C. At regular time intervals an aliquot of 2 mL of supernatant was withdrawn for arsenic analysis. The pseudo-second-order *kinetic* model can be solved with the following equations. The kinetic rate equation is expressed as

$$dq_t/dt = k_2(q_{eq} - q_t)^2 \tag{3}$$

where q_{eq} is the sorption capacity at equilibrium and q_t is the solid-phase loading of arsenic at time t. k_2 (mL·mg^{-1}·h^{-1}) represents the pseudo-second-order rate constant for the kinetic model (*40*, *49*). By integrating eq 3 with the boundary conditions of $q_t = 0$ at $t = 0$ and $q_t = q_t$ at $t = t$, the following linear equation can be obtained:

$$\frac{t}{q_t} = \frac{1}{V_0} + \frac{1}{q_{eq}}t \tag{4}$$

$$V_0 = k_2 q_{eq}^{\ 2} \tag{5}$$

where V_0 (mg·mL^{-1}·h^{-1}) is the initial sorption rate. Therefore, the V_0 and q_{eq} values of kinetic tests can be determined experimentally by plotting t/q_t versus t.

Effects of pH on Arsenic Removal. A 50 mL portion of arsenic solution and 1 mL of BCF were added to a 250 mL conical flask. The initial arsenic concentration was 300 mg/L, and the pH was in the range of 4−11. All samples were set in a to-and-fro shaker at 150 rpm at 25 ± 0.5 °C. The samples were adjusted for several times till the desired pH was reached and stable. After 24 h aliquots of the samples were withdrawn for arsenic analysis.

Effects of Competing Anions on Arsenic Removal. A 1 mL portion of BCF and 50 mL of arsenic solution in the absence and presence of PO_4^{3-}, SiO_3^{2-}, and SO_4^{2-} were added to a 50 mL conical flask. The initial arsenite and arsenate concentrations were 4 and 2 mmol/L, respectively. The competing anions prepared from potassium salt were at the same molar concentration as arsenic. All samples were shaken in a to-and-fro shaker at 150 rpm at 25 ± 0.5 °C. The pH of the supernatant was adjusted to 7.0 ± 0.1 by a small volume of 0.1 mol/L HCl or NaOH solution. After 24 h of shaking, the samples were withdrawn for arsenic analysis.

Column Experiments and Regeneration. Column experiments were conducted using a glass column of 10 × 400 mm packed with a determinate volume of BCF. Deionized

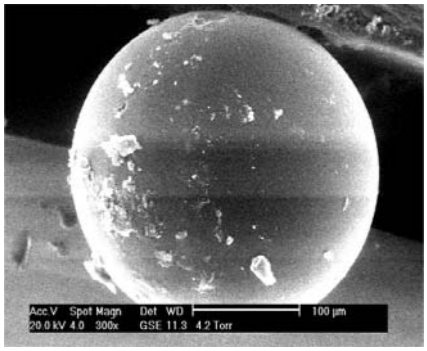

FIGURE 1. ESEM micrograph of BCF.

water or groundwater collected from a well in Jixian, China, supplemented with 500 μg/L arsenic, was used as the feed solution. The feed solution used was prepared two times per day to guarantee the stability of the arsenic species. Tap water was pumped through the packed column with a peristaltic pump (HL-1S, Shanghai Huxi Analytical Instrument Co., China). For As(III) column runs, a black plastic shield was used to avoid the solar oxidation of As(III) to As(V).

When the effluent arsenic concentration was higher than 50 μg/L, BCF was withdrawn from the column and collected in a 250 mL flask for regeneration. A 2 mol/L NaOH solution corresponding to 10 times the BCF volume was added, the suspension was shaken at 150 rpm and 25 $\pm$ 0.5 °C for 5 h, and then the alkaline solution was dumped out. The desorption process was repeated four times, and BCF treated with alkaline solutions was eluted with deionized water several times.

Analytical Procedures. BCF covered with arsenic was digested by $HNO_3-HClO_4-H_2SO_4$ (10:3.5:2.5). The digested solution was then diluted for arsenic analysis by flow injection−hydride generation atomic fluorescence spectrophotometry (FI−HG-AFS) (*53*) (CAFS230, Haiguang Corp., Beijing). The arsenic detection limit of this method was 0.1 μg/L, and the analytical regression coefficient γ^2 was >0.9990. The shape of BCF was observed with an environmental scanning electron microscope (Phlilps, XL30ESEM, Holland). The speciation of iron oxyhydroxide loaded in BCF was detected with an X-ray diffraction analysis instrument (D/Max-2500, Japan). The crystal shape of β-FeOOH loaded in BCF was observed with a scanning electron microscope (Hitachi, 5-3500W, Japan). BCF was digested by $HNO_3-HClO_4-H_2SO_4$ (10:3.5:2.5), and the digested solution was diluted to a certain Fe concentration that could be detected with a UV spectrophotometer at 510 nm (*53*) (UV 754, Shanghai Precision Scientific Instrumental Co., Shanghai). The background ion concentrations of groundwater were detected with an ion chromatograph (Diome Co., DX-120).

Results and Discussion

Characterization of BCF. An ideal adsorbent compatible with fixed-bed column processes should have a spherical shape, excellent mechanical strength, and attrition resistance properties. Figure 1 shows the environmental scanning electron microphotograph of a random bead. As seen from the microphotograph, the beads were absolutely spherical under wet conditions. They remained spherical even after a long time of attrition under a certain pressure. This indicated BCF had ideal mechanical strengths and attrition resistance properties.

To examine the iron mineral phase loaded in BCF, the samples were detected by X-ray diffraction (XRD). The XRD pattern of the adsorbent is presented in Figure 2. Figure 3 shows that the iron oxyhydroxide loaded in BCF was mainly

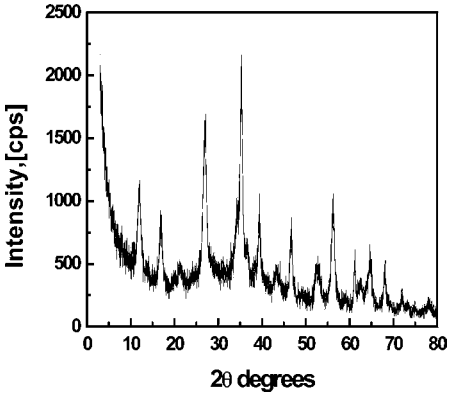

FIGURE 2. X-ray diffraction patterns of BCF.

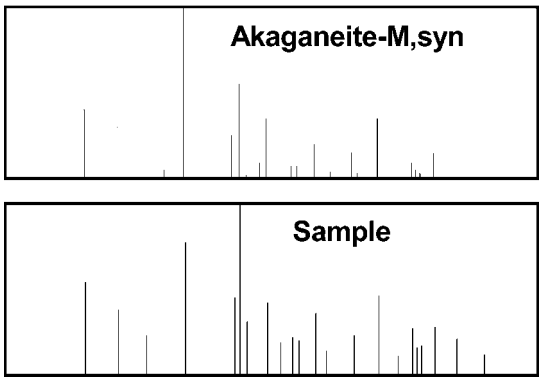

FIGURE 3. Comparison of X-ray diffraction peaks between BCF and standard β-FeOOH.

in the form of akaganéite (β-FeOOH). The crystals loaded in BCF were observed by scanning electron microscopy, and the micrographs showed that the diameter of the Fe mineral phase in BCF was about 200−300 nm except for a few micrometer level particles. Our experiments demonstrated that if the Fe loading was conducted in 0.1 mol/L HAc−Ac^- (pH 5.0) buffer solution, the Fe mineral phase existed as goethite, which had only half the adsorption capacity for arsenic compared to akaganéite. Reports showed akaganéite had higher arsenate adsorption capacity than other Fe mineral phases such as hydrous ferric oxide, am-FeOOH, and goethite too (*54*). It can be concluded that akaganéite is an advantageous species for removal of arsenic compared with other Fe mineral phases.

Cellulose is a linear polymer of β-(1,4)-D-glucopyranose units in the $^4C_1$ conformation. Each glucose unit has three hydroxyls. The oxygen of the hydroxyls on the glucose units might bond with Fe ions. Hydroxyls might contribute to the formation of the first layer of the Fe mineral phase, akaganéite, at the surface of the cellulose polymer through the hydrolization of Fe ions while the alkaline solutions were slowly dropped into. And then new crystalloids assembled continuously and automatically surrounded the formed akaganéite while the loading process was continued. XRD indicated that the residual Fe mineral phase suspended in the supernatant liquid after the loading process was amorphous iron hydroxide. This indirectly illustrated the cellulose contributed to the formation of akaganéite in the interior surface of cellulose beads too. However, further research is needed to study the mechanisms by which cellulose contributes to the formation of akaganéite.

Maximum Fe Content Loaded in BCF. The adsorption capacity for arsenic is strongly dependent on the species and content of the reactive components and the category and characteristic of the carriers. The content of iron is a crucial factor to impact the arsenic adsorption capacity for

TABLE 1. Comparison of Maximum Fe Loaded in Different Adsorbents

carrier	max Fe (mass %)	Fe speciation	ref
cotton cellulose beads	50	β-FeOOH	this study
polystyrene (SO_3^-)	9−12	FeOOH	*36*
chelating resin	5	Fe(III)	*37*
polystyrene and polyHIPE	7−7.5	hydrous iron oxides	*38*
iron oxide-impregnated activated carbon	7	iron oxides	*20*
sand	0.1−0.2	hydrous iron oxides	*25*
sand	2−3	hydrous iron oxides	*17*

adsorbents loaded with iron. The amount of iron loaded in the bead cellulose was determined by treating the bed with HCl or HNO_3 (10 mL)−$HClO_4$ (3.5 mL)−H_2SO_4 (2.5 mL), which recovered all the loaded iron, and the resulting solution was analyzed for iron concentration and correlated with the volume of cellulose beads from which it was derived. Table 1 lists the highest content of iron loaded in the variety of carriers. The highest iron coated on sand was between 1−2 and 20−30 mg of Fe/g of sand (*17*, *25*). There was a significant increase in the amount of iron coated on the surface of polystyrene beads when the initial ferric nitrate concentration was increased from 0.025 to 0.1 M. The highest content of iron oxides coated on the surface of polystyrene beads was 70−75 mg of Fe/g. When the initial ferric iron concentration was above 0.1 M, the amount of coated iron did not show any significant increase (*38*). The sand particles and polystyrene beads used were solid in structure without macro- or mesopores, so that the amount of iron oxides coated on the surface of the carriers was very limited. PolyHIPE foam was a highly porous material, so it could give the possibility for iron hydroxides to penetrate into the interior of the polymer structure, apart from producing an outer surface coating as in the case of polystyrene beads and amorphous sands. Therefore, the iron amount on polyHIPE increased significantly compared with that on solid polystyrene beads (*38*). Iron oxides could be uniformly loaded into the carriers with a relatively high content of iron if the media were not only highly porous, but also presented with adsorption sites for Fe(III). For example, macroporous polystyrene beads, functionalized with a high concentration of sulfonic acid groups, could be loaded with 9−12% Fe mass (*36*). Currently, an iron oxide impregnated activated carbon was applied for the removal of arsenate, and the iron accounted for 7% in mass (*20*).

Compared with the reported carriers only loaded with a 0.1−12% maximum content of Fe which was relatively less stable (e.g., sand), the highest amount of iron loaded in the cellulose beads in this study was found to be 360 mg/mL (50% in mass), which was much higher than that of the reported adsorbents. This could be attributed to the carrier's chemical and physical properties, and the innovative method to realize the loading process. In terms of physical properties, cellulose was distinguished from other carriers (e.g., sand, resin, zeolite, silica, and activated carbon) by its hydrophilicity, high porosity (85%), and high surface area. As for the chemical properties, the possible situation was that hydroxyls, which made the media highly hydrophilic, had strong affinity toward Fe(III). Furthermore, the loading process of Fe in the cellulose beads could be continuously repeated several times till saturation through hydrolization of ferric salts when alkaline solution was added dropwise.

The loading efficiency of iron on BCF decreased with increasing loading time. This trend was especially significant when the loading process approached the saturation level. The loading efficiency was sustained above 90% till the iron coverage of 220 mg/mL. Therefore, BCF covered with 220 mg/mL iron was used in the following experiments, including determination of arsenate adsorption isotherms and kinetics, determination of the effect of pH and competing ions, column experiments, and regeneration.

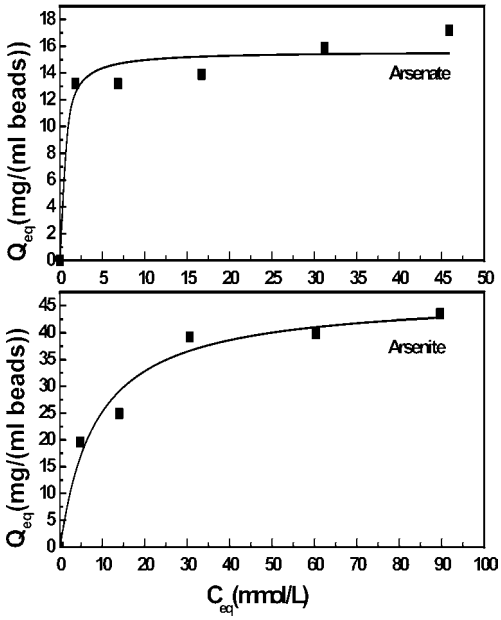

FIGURE 4. Adsorption isotherms for arsenite and arsenate by bead cellulose adsorbents loaded with Fe(β-FeOOH) (temperature 25 ± 0.5 °C, pH 7.0 ± 0.1, Fe content of BCF 220 mg/(mL of beads), liquid: solids = 50 mL:1 mL).

TABLE 2. Langmuir and Freundlich Adsorption Isotherm Parameters for Arsenite and Arsenate by BCF

	Langmuir			Freundlich		
As species	b	Q_{max} (mg/mL)	r^2	K	n	r^2
arsenate	2.29	15.6	0.96	11.7	11.5	0.98
arsenite	0.120	46.8	0.97	13.5	3.74	0.97

	Fe content		Q_{max} of As		max As/Fe
As species	mg/mL	mg/g	mg/mL	mg/g	(mol/mol)
arsenate	220	468	15.6	33.2	0.053
arsenite	220	468	46.8	99.6	0.16

Arsenic Adsorption Isotherms. To investigate the adsorption capacity, a series of arsenite and arsenate solutions were shaken with the adsorbent BCF for 24 h. Figure 4 shows the adsorption isotherms of arsenite and arsenate on BCF at pH 7.0. In this study, Langmuir and Freundlich isotherms have been applied. Adsorption data fit Langmuir and Freundlich isotherms well (r^2 > 0.96), and adsorption constants evaluated from the isotherms at certain experimental conditions are listed in Table 2. High correlation coefficients suggested that both models were suitable for describing the adsorption equilibrium of arsenite and arsenate by BCF. For the Freundlich equation, the constant K is an indication of the adsorption capacity of the adsorbent, while the parameter n indicates the effect of concentration on the adsorption capacity and represents the adsorption intensity. The magnitude of K and n values showed the easy uptake of arsenic species and the high adsorptive capacity of BCF.

The Freundlich model does not describe the saturation behavior of the adsorbent, whereas the Langmuir constant represents the monolayer saturation at equilibrium. Constant

b corresponds to the concentration at which arsenic species in an amount equal to $Q_{max}/2$ are bound. In this case, the high value of b also implied strong bonding of arsenite and arsenate to BCF at ambient temperature. Q_{max} is the maximum value of q_{eq} that is most important to identify the adsorption capacity. The density of BCF, Fe content, and maximum arsenic adsorption capacity divided by wet volume and dry mass are listed in Table 2. Determined from the Langmuir equation, the maximum adsorption capacity for arsenite and arsenate by BCF was 46.8 and 15.6 mg/mL (99.6 and 33.2 mg/g), respectively, at equilibrium pH 7.0. Iron oxides, including amorphous iron hydroxide, ferrihydrite, and goethite, showed higher adsorption capacity for arsenite than for arsenate in other studies (*12*, *18*). In consideration of the adsorption capacity for arsenic, BCF appears to be much superior to activated alumina and activated carbon. BCF showed much greater capacity for As(III) compared with iron oxide-coated sand ($Q_{max} = 0.043$ mg/g) (*55*) and activated alumina ($Q_{max} = 3.5$ mg/g) (*10*). The maximum adsorption for As(V) by BCF was 2 and 7 times that on activated alumina and activated carbon loaded with Fe, respectively (*56*, *57*). The fact that BCF showed much higher arsenic adsorption capacity than the commonly reported adsorbents above could be attributed to the high content of iron loaded, an appropriate iron mineral phase (β-FeOOH), and a cellulose carrier with high porosity and hydrophilility. The maximum As/Fe ratios for arsenite and arsenate were 0.053 and 0.16, respectively. It was reported that the maximum adsorption density of arsenate by akaganéite nanocrystals was 0.16 mol_{As} mol_{Fe}^{-1} (*54*). The lower maximum adsorption density by BCF compared to akaganéite nanocrystals could be attributed to the lower surface area and micrometer distribution in particle size. In this connection, it could be stated that the adsorption capacity for arsenic should be increased greatly if iron oxyhydroxide were loaded as nanometer particles. However, better impregnation techniques should be developed to disperse the nanometer iron oxyhydroxide into the cellulose media.

As for the mechanisms by which As(III) and As(V) are adsorbed on akaganéite, previous spectroscopic studies show that arsenic is adsorbed to iron oxyhydroxides by forming inner sphere surface complexes by ligand exchange with hydroxyl groups at the mineral surface (*32*, *33*). To study the mechanism of adsorption process, we measured extended X-ray absorption fine structure (EXAFS) spectra of arsenic adsorbed to BCF. The results showed that the dominant complexes were bidentate binuclear corner-sharing between the AsO_4 tetrahedra of arsenic species and FeO_6 octahedra of iron oxyhydroxide loaded in BCF. Besides the adsorption reaction, there was no change in oxidation state following interaction between the arsenic species and BCF.

Kinetics of Arsenic Removal. The kinetics of sorption that describes the solute uptake rate governing the residence time of the sorption reaction is one of the important characteristics that define the efficiency of sorption. Hence, in the present study, the kinetics of arsenic removal was determined to understand the adsorption behavior of BCF. Figure 5A shows the adsorption data of arsenic by BCF at different time intervals and the simulation to the pseudo-second-order kinetic model. As seen in Figure 5A, the adsorption of As(III) and As(V) to BCF was found to be time dependent. The adsorption of arsenite and arsenate was rapid for the first 2 h, when the elimination rate reached 70% and 30%, respectively, and then slowed considerably. For arsenite, the removal rate was 90% after 6 h and the adsorption equilibrium was approached. The removal rate for arsenate reached 77% in 10 h, and the adsorption approached equilibrium too. From the kinetic results, the higher percentage removal of arsenite than that of arsenate is consistent with adsorption isotherm tests. Arsenic was initially adsorbed

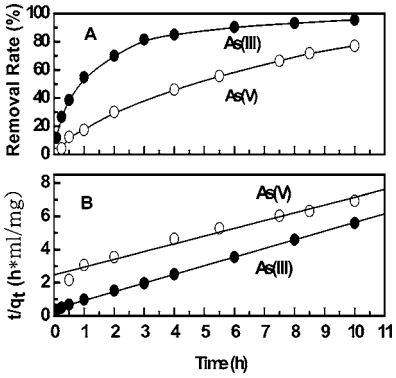

FIGURE 5. Kinetics of arsenic adsorption by BCF: (A) arsenic removal rate versus t; (B) transformation with t and t/q_t (temperature 25 ± 0.5 °C, initial pH 7.0 ± 0.1, Fe content of BCF 220 mg/(mL of beads), initial [As] = 7.5 mg/L, liquid:solids = 250 mL:1 mL).

TABLE 3. Parameters of a Pseudo-Second-Order Kinetic Model Fitting Arsenic Adsorption Kinetics

As species	V_0 (mg·mL^{-1}·h^{-1})	q_{eq} (mg/(mL of beads))	k_2 (mL·mg^{-1}·h^{-1})	r
arsenite	2.43	1.92	0.66	0.999
arsenate	0.405	2.14	0.09	0.986

by the exterior surface of the BCF. When the adsorption at the exterior surface reached the saturation level, the arsenic ions began to enter the BCF via the pores within the particles and were adsorbed by the interior surface of the particles. When the arsenic ion diffused into the pores of the BCF, the diffusion resistance was increased, which in turn led to a decrease in diffusion rate. With the decrease in arsenic concentration in the solution, the diffusion rate became constantly lower, and consequently, the diffusion processes reached equilibrium.

It has been reported that activated alumina adsorption kinetics was typically slow and that up to 2 d was required for the adsorption of arsenic to 100 mesh activated alumina grains to reach half the equilibrium value (*19*). The faster adsorption of arsenic by BCF than by activated alumina has significant practical importance as it will shorten the reaction time and consequently increase the efficiency. The fast sorption ability can be attributed to both the physical and chemical properties of BCF. In terms of physical properties, cellulose beads have high hydrophilicity, high porosity, relatively uniform pore size, and high surface area. As for chemical properties, akaganéite, which is uniformly loaded into the cellulose beads, adsorbs arsenic with high adsorption kinetics.

Figure 5B is the plot of t versus t/q_t to determine the V_0 and q_{eq} values for all media. The correlation coefficients (r) and several parameters obtained from the pseudo-second-order kinetic model are shown in Table 3. The pseudo-second-order model fits the kinetic data of BCF very well, indicating very high determination coefficients of above 0.99. The initial adsorption rate of arsenite is 2.43 mg·mL^{-1}·h^{-1}, which is 6 times greater than that of arsenate (0.405 mg·mL^{-1}·h^{-1}). Kim (*49*) reported that mesoporous aluminia adsorbed arsenate 2 times faster than arsenite in 1 h and attributed it to the smallness of the radius of an arsenate ion (4.0−4.2 Å) compared with that of an arsenite ion (4.8 Å) in water. But the different results from Matsunaga (*37*) showed that arsenite adsorption by iron(III)-loaded chelating resin reached equilibrium in 2 h while at least 5 h was required for arsenate. Raven et al. (*12*) reported arsenite adsorption by ferrihydrite was considerably faster; i.e., approximate equibibrium was achieved sooner than with arsenite, with

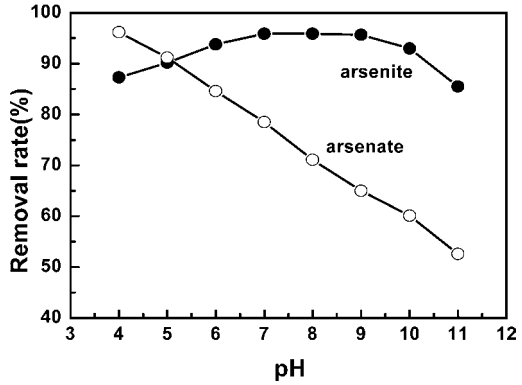

FIGURE 6. Arsenic removal by BCF vs pH (temperature 25 ± 0.5 °C, Fe content of BCF 220 mg/(mL of beads), initial [As] = 300 mg/L, liquid:solids = 50 mL:1 mL).

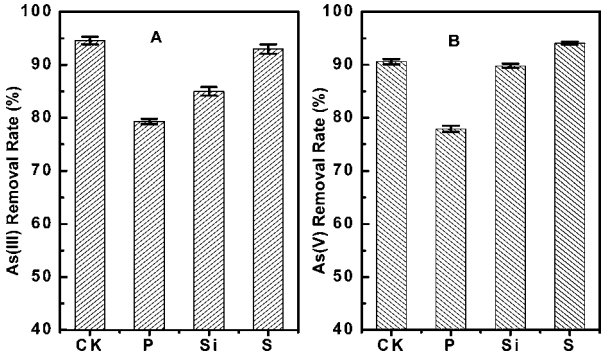

FIGURE 7. Effect of competing anions on arsenic removal by BCF: (A) arsenite; (B) arsenate (temperature 25 ± 0.5 °C, equilibrium pH 7.0 ± 0.1, Fe content of BCF 220 mg/(mL of beads), [As(III)] = 300 mg/L and competing anions concentration 4 mmol/L, [As(V)] = 150 mg/L and competing anions concentration 2 mmol/L, liquid:solids = 50 mL:1 mL; CK = control, P = PO_4^{3-}, Si = SiO_3^{2-}, S = SO_4^{2-}).

an initial arsenic solution concentration equivalent to 13.3 mol_{As} kg^{-1}. The results from this study are consistent with reports of Matsunaga (*37*) and Raven (*12*). The reason arsenite is adsorbed faster than arsenate by BCF is not clear yet. Unlike arsenite, in which the supernatant pH was stable, the pH increased from 7 to 12 for arsenate equilibrium solution. This indicates that hydroxide ions were released in the adsorption process.

Effects of pH on Arsenic Adsorption. To determine the optimum pH for adsorption of arsenic over BCF, the uptake of arsenic as a function of pH was studied. Removal of arsenic in the range of pH 4−11 is shown in Figure 6. In general, the removal rate of arsenate decreased with increasing pH. The percent removal of arsenate by BCF was reduced from 96.2% to 52.6% as pH shifted from 4 to 11. In the wide pH range, the percentage removal of arsenite by BCF was higher than that of arsenate except for pH 4−5. This accorded with the results of adsorption isotherms and kinetics. In comparison with arsenate, arsenite was preferably adsorbed by BCF in a wide pH range of 5−11. The percent removal of arsenite was above 90% in the range of pH 5−10. Optimal arsenite adsorption by BCF was found in the range of pH 7−9 in which the removal rate was above 95%.

pH affects significantly the speciation of arsenic in solution and the surface charge of the solid particles. Arsenate species and their corresponding stability pH values are H_3AsO_4 (pH < 2), $H_2AsO_4^-$ (pH 2−7), $HAsO_4^{2-}$ (pH 7−11), and AsO_4^{3-} (pH > 12). On one hand, as pH increased from 4 to 11, the amount of multivalent species ($HAsO_4^{2-}$ (pH 7−11) and AsO_4^{3-} (pH > 12)) increased and the two species were not preferably adsorbed by BCF in comparison with $H_2AsO_4^-$. On the other hand, to interpret the experimental data using amphoteric dissociation theory, the value of pH_{PZC} is needed where the surface charge is zero. Iron oxides, whether they can be identified as having a particular crystal structure or not, typically have PZCs in the pH range 7−9 (*38*). Deliyanni et al. (*54*) reported the pH_{PZC} of nanocrystalline akaganéite was initially 7.3 and decreased to about 6 when arsenate was adsorbed. Similar to that of nanocrystalline akaganéite, the pH_{PZC} value of BCF should also decrease due to the release of hydroxide ions in the adsorption process of arsenate. The surface of BCF is positively charged when the equilibrium pH values are below pH_{PZC}, but the positively charged sites decrease with increasing pH. And then it will be negatively charged when the equilibrium pH increases above pH_{PZC}. As the equilibrium pH increased from lower pH to pH_{PZC}, the decreased percentage removal of arsenate was attributed to the decreasing electrostatic attraction between the surface of iron oxyhydroxide loaded in BCF and anionic arsenate species. Over the PZC value, the surface sites of BCF were negatively charged and inappropriate for adsorbing anionic arsenate species. The lower adsorption of arsenate at pH > pH_{PZC} could be due to an increased repulsion between the negatively charged arsenate species and negatively charged surface sites. Similar results were also obtained by Raven et al. (*12*), who investigated the adsorption of arsenate on ferrihydrite at high arsenate concentration.

Trivalent arsenic is stable as neutral H_3AsO_3 at pH < 9, while $H_2AsO_3^-$, $HAsO_3^{2-}$, and AsO_3^{3-} are stable species in the pH ranges of 9−12, 12−13, and >13, respectively. Since arsenite species have less negative charge character as compared to arsenate species in the pH range 4−9, they do not exhibit as much repulsion, and as a result, arsenite was preferably adsorbed by BCF in a wide pH range. In the pH range 4.0−9.5, the predominant species are H_3AsO_3 and $HAsO_3^{2-}$. As pH increases, the amount of negatively charged arsenic species rises while the positively charged surface sites decrease up to pH_{PZC}. In this connection, it can be stated that arsenite can be adsorbed through specific adsorption between the neutral species and positively charged surface sites at lower pH values. The decrease in the adsorption yield above pH 9 may be attributed to an increase of negatively charged arsenite species and negatively charged surface sites. Favorable adsorption of arsenite on kaolinite, illite, montmorillonite, and amorphous aluminum hydroxide was also reported in the pH range of 7.5−9.5 by Manning et al. (*15*). Raven et al. (*12*) also reported an optimal adsorption at pH 7.0−9.5 between arsenite and ferrihydrite at high arsenite concentration.

Arsenite was preferably adsorbed by BCF in a wide pH range. Although optimal arsenate removal was found in acidic conditions, high removal performance was still observed near the neutral pH at a high initial concentration of arsenate. The character of arsenic removal responding to pH variation has great significance in application. In general, the solution pH of natural water is in the range of 6−8.5, so the pH preadjustment is not needed for the contaminated groundwater when BCF is applied in the removal of arsenic.

Effects of Competing Anions. In groundwater sources several anionic components might exist, which could compete with arsenic for the available adsorption sites. Among the major coexisting anionic components, phosphates, silicate, and sulfate are usually present in groundwater streams, possibly inhibiting arsenic removal by BCF. To investigate the effect of the above competing anions on arsenic removal, arsenic solutions were spiked with competing anions and the removal of arsenic was determined. Figure 7 shows the effects of competing anions (PO_4^{3-}, SiO_3^{2-}, and SO_4^{2-}) on arsenic removal. The removal rates for arsenite and arsenate were 94.6% and 90.6%, respectively, in the control at initial As concentrations of 300 and 150 mg/L. The

presence of phosphate reduced the arsenite removal rate by 15% as compared with that of the control. The removal rate of arsenite decreased to 85% in the presence of silicate, indicating less influence of silicate on adsorption of arsenite by BCF than that of phosphate. Similar to that of arsenite, arsenate removal was reduced greatly (13%) in the presence of phosphate. Considering the experimental error, the effect of silicate on arsenate removal was not significant. Sulfate, which is a common competing anion in groundwater, did not evidently decrease the removal efficiency of both arsenite and arsenate.

Both phosphate and silicate bonded with β-FeOOH and competed for adsorption sites with arsenic. Previous studies (*58*, *59*) showed that arsenic was adsorbed as an inner sphere complex on iron oxyhydroxides. Phosphorus and arsenic have similar atomic structures and chemical properties. They have atomic numbers of 15 and 33, sharing the same outer shell of s^2p^3. Phosphate and arsenic always compete with each other in both natural solids and biological systems (*3*). The reason that phosphate greatly impacted the removal of arsenic by BCF could be that phosphate had chemical characteristics very similar to those of arsenic and cooperated with iron oxyhydroxide crystals by forming an inner sphere complex too (*60*). In comparison with PO_4^{3-}, SiO_3^{2-} showed moderate and no effects on the removal of arsenite and arsenate by BCF. This indicated that BCF had higher affinity for arsenic than for silicate. Similar results were obtained by Meng et al. (*8*), who studied the silicate effects on the removal rates of arsenite and arsenate by iron hydroxides. It is still being argument whether sulfate forms an outer or an inner sphere complex at the surface of the iron oxyhydroxide/water interface (*61*). The fact is clear that adsorbed sulfate has less affinity than phosphate ions for iron oxyhydroxides (*61*). In this study, the presence of SO_4^{2-} had no impact on the adsorption of arsenic by BCF.

The effects of competing anions on arsenic removal were dependent on the type of anions, the solution pH, and the concentration of interfering ions and arsenic in the solutions. The effects of phosphates, silicate, and sulfate were investigated because they are usually present in groundwater streams, possibly inhibiting arsenic removal, whereas the effects of chloride and nitrate were ignored due to the very low affinity of chloride for iron oxyhydroxides. In this test, pH 7.0 was chosen since the pH of the natural water is generally near neutral. To avoid complete removal of arsenic, which could induce the effects of competing anions to be hidden by a low concentration of spiked arsenic and competing anions, the initial concentrations of arsenic and competing anions designed in the test were much higher than in natural groundwater. Katsoyiannis et al. (*38*) reported the interfering effects of phosphate on the removal of arsenic by iron oxide-coated polymeric materials increased with increasing phosphate concentration, and when natural waters contained a limited amount of phosphates, they did not show any significant inhibition on arsenic removal. Similar results were obtained by Wilkie et al. (*21*), who investigated the effects of sulfate and phosphate on the removal of arsenic by hydrous ferric oxide. Therefore, it is suggested that the effects of phosphate and silicate on arsenic removal by BCF would decrease from those in natural groundwater considering the concentrations of arsenic and interfering ions are much below the designed level in this test. These trends should have been approved by the following column runs in which the groundwater contained common concentrations of interfering ions.

Fixed-Bed Column Runs. (1) Arsenic Breakthrough Behavior from Deionized Water. The practical way to design an adsorption column is to conduct experiments with a laboratory column. Figure 8 shows breakthrough behavior during fixed-bed column runs from deionized water supplemented with arsenic. At an EBCT (empty-bed contact time) of 3.0 min, the arsenite effluent concentration was below 2 μg/L until the empty-bed volume reached 1500, and achieved breakthrough at 2000 empty-bed volume (BV) according to WHO's arsenic maximum contaminant level (MCL, 10 μg/L). At an EBCT of 3.2 min, the arsenate concentration in the effluent solution was above 10 μg/L when the effluent volume reached 300 BV and was later maintained at 20−40 μg/L in the range of 500−3000 BV. According to Bangladesh's arsenic MCL (50 μg/L), the breakthrough for As(III) and As(V) was not observed even when the bed volumes reached 3500 at an EBCT of 3.0−3.2 min. The batch experiments described above showed the adsorption capacity for arsenite by BCF was about 3 times that of arsenate at neutral pH. The results that BCF showed higher removal performance for As(III) than for As(V) in column experiments accorded with the adsorption isotherm study. Arsenite is the predominant species under reducing conditions such as groundwater. Bangladesh is one of the most serious arsenic-contaminated countries, where the typical proportion of arsenite appears to be between 50% and 60% of the total As (*62*). In each area of Chinese Taiwan, the groundwaters are likely to be strongly reducing, a hypothesis supported by the observation that As is present largely as As(III) (*63*). Most of the reported adsorbents were not effective for As(III) removal unless As(III) was preoxidized by chlorine, manganese dioxide, ozone, or other innocuous oxidizing agents. The characteristic of high removal performance for As(III) met with the requirement of arsenic species distribution and indicated that BCF did not warrant any preoxidation treatment before the column runs.

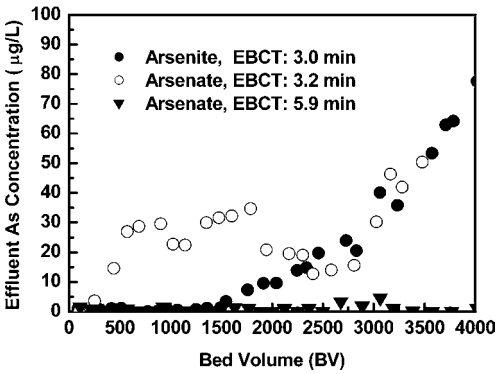

FIGURE 8. Arsenic breakthrough behavior of the column test from deionized water. (temperature 25 ± 0.5 °C, influent pH 7.0 ± 0.1, Fe content of BCF 220 mg/ mL, initial [As] 500 μg/L, As(III) EBCT = 3.0 min and SLV (superficial liquid velocity) = 1.72 m/h, As(V) EBCT = 3.2 min and SLV = 2.43 m/h, As(V) EBCT = 5.9 min and SLV = 1.32 m/h).

Further investigation regarding the treatment efficiency included the examination of operational parameters, such as EBCT. EBCT is a critical parameter when adsorption experiments are involved because the removal efficiency depends strongly on the contact time between the adsorbent (BCF) and adsorbate (arsenic). The removal efficiencies of arsenate were investigated at EBCTs of 3.2 and 5.9 min. As expected, EBCT evidently affected the breakthrough behavior, and the adsorptive efficiency increased with increasing EBCT, due to the resulting higher contact time. At an EBCT of 5.9 min, the As(V) remaining in solution was continuously below 5 μg/L even when the effluent volume reached 4000 BV, while breakthrough (MCL, 10 μg/L) was observed as 300 BV at an EBCT of 3.2 min. When adsorption was used as an available method to remove the pollutants from aqueous systems, the empty-bed contact time of the influent was generally 1.5−12 min (*64*). Relatively being a shade worse compared with that of arsenite, the removal performance of arsenate was still

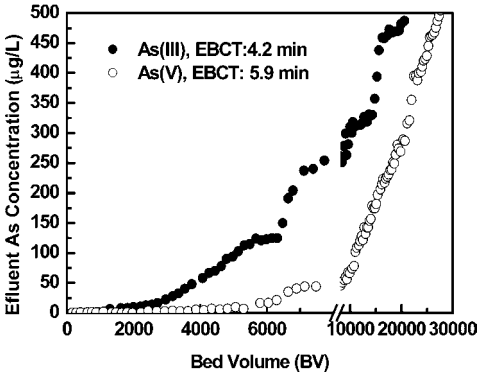

FIGURE 9. Arsenic breakthrough behavior of the column test from groundwater. (temperature 25 ± 0.5 °C, influent pH 7.0 ± 0.1 for As(V) and 8.2 for As(III), Fe content of BCF 220 mg/mL, influent [As] = 500 μg/L, As(III) EBCT = 4.2 min and SLV = 2.07 m/h, As(V) EBCT = 5.9 min and SLV = 1.47 m/h).

noteworthy since the breakthrough (10 μg/L) empty-bed volume was above 4000 at relatively higher influent As(V) concentration (500 μg/L) and shorter EBCT (5.9 min).

(2) Arsenic Breakthrough Behavior from Groundwater. Dynamic experiments using natural groundwater as feedwater are necessary to predict BCF behavior in a treatment process and its ability to remove arsenic to a drinking level. Figure 9 shows the breakthrough behavior of arsenic from natural groundwater during the first column runs. EBCT for the As(V) column was designed longer than that of As(III) with respect to the lower removal performance for As(V). At EBCTs of 4.2 and 5.9 min, breakthrough empty-bed volumes at the WHO provisional guideline value of 10 μg/L for As(III) and As(V) were 2200 and 5000, respectively, corresponding to 2.3 and 5.2 mg of As/(g of solids) breakthrough solid-phase concentrations. Breakthrough was observed at 4000 and 8500 BV according to the MCL of 50 μg/L, which was practiced in Bangladesh. When the effluent solute concentration reaches 95% of its influent value, it is usually called the point of column exhaustion, at which the solid-phase concentration reaches a maximal value. The maximal retention capacities for As(III) and As(V) were 12.9 and 18.7 mg of As/(g of solids), resulting from integrating the breakthrough behavior by Origin 6.0. It should be noted that the maximal retention capacities were much below the maximum adsorption capacities obtained in batch experiments. This can be explained by the relatively higher flow rate in the column experiments, which may not provide sufficient contact time between BCF and arsenic. Breakthrough empty-bed volume is dependent essentially on EBCT and influent arsenic concentration. It should be larger at lower initial arsenic concentration and longer EBCT. Considering the higher sensitivity for As(III) than for As(V), BCF might treat greater volumes of As(III) bearing water than that of As(V) at equal operating conditions in the column experiments.

It has been suggested that activated alumina could be applied successfully for removing arsenic if the influent pH were slightly acidic and the competing anions were present in small concentration (e.g., <0.1 mg/L) (*57*). For activated alumina sorption, pH adjustment through acid dosage was required to achieve high arsenic removal capacity (*57*). Compared with activated alumina, BCF also removed more arsenate in acidic conditions, while the adsorption capacity was noteworthy too in neutral pH. The column experiments showed that BCF still sustained high arsenate removal efficiency in neutral pH. For arsenic-laden groundwater with a low sulfate content, ion exchange had the potential to be a viable process, but the pH and alkalinity of the product water decreased significantly during the initial period of the column run for tens of bed volumes, thus necessitating posttreatment pH adjustment (*36*). BCF did not change the pH of As(III)-laden waters, and the postadjustment of pH was not needed for As(V), considering the effluent pH had only increased 0.4 unit. What most limited the application of anion exchanger was that it preferred sulfate over arsenate. Therefore, the arsenate removal capacity was greatly reduced in the presence of a high concentration of competing sulfate ions (*36*). As seen from the batch experiments, the presence of sulfate had no impact on the adsorption of arsenic by BCF. In the column experiments, 15.2 mg/L sulfate ions in the groundwater did not significantly affect the removal efficiency of arsenate and arsenite by BCF either. Neither polymeric anion exchanger nor activated alumina was effective for As(III) removal. It was necessary to introduce a preoxidation step before using the two adsorbents. Preoxidation treatment posed operational complexity and diminished the overall viability of the fixed-bed process. Distinguished from anion exchanger and activated alumina, BCF was very sensitive to both arsenite and arsenate and exhibited excellent arsenic removal without any preoxidation of the influent. When 1 mg/L As(III)- and As(V)-laden water flowed through iron oxide-coated sand at an EBCT of 50 min, breakthrough empty-bed volumes at an arsenate concentration of 10 μg/L were in the ranges 163−184 and 149−165 per cycle, respectively (*65*). Even in the thermal treatment procedure, the significant detachment of iron from the sand particles was observed in the effluent during column studies (*55*). The breakthrough point was reached after almost 18 and 34 treated bed volumes for arsenite and arsenate, respectively, while the solid polystyrene beads loaded with iron hydroxides were applied for the removal of arsenic at an EBCT of 25 min and 50 μg/L supplemented arsenic (*38*). PolyHIPE foam was a highly porous material, which could give the possibility for iron hydroxides to penetrate into the interior of the polymer structure, apart from producing an outer surface coating as in the case of polystyrene beads and amorphous sands. The breakthrough point increased to 250 treated bed volumes in comparison with that of polystyrene beads (*38*). A commercially available macroporous cation exchanger with a polystyrene matrix and sulfonic acid functional groups was used as the parent cation exchanger. The spherical polymer beads were dispersed interiorly with crystalline and amorphous hydrous ferric oxide microparticles after a three-step procedure. Arsenite and arsenate breakthroughs (10 μg/L) were observed after 2000 and 4000 BV, respectively, while influents flowed through this hybrid ion exchanger adsorbent (HIX) supplemented with 50 and 200 μg/L arsenic species at EBCTs of 3.1 and 4.0 min (*36*). Compared to polystyrene beads, PolyHIPE foam, and HIX, which were produced from polymeric materials, the raw material for preparing BCF came from cotton cellulose, which was sustainable and reproducible. The most important significance for BCF was that it had much higher removal performance than the three polymers listed for both arsenite and arsenate in the column experiments. Conclusively, BCF showed a significant advantage in comparison with other adsorbents: high selectivity toward both As(III) and As(V) species and no additional pre- or posttreatment (e.g., pH adjustment, preoxidation).

(3) Recycle of BCF. For the sorption process to be viable, BCF has to be amenable to efficient regeneration and reuse. Figure 10 shows breakthrough behavior of arsenic during four cycles of column run from groundwater collected from a well in Jixian, Tianjin, China. The regeneration was conducted by shaking exhausted BCF in 8% alkaline solution four times. And then regenerated BCF was eluted with deionized water several times. Analytical determinations showed that more than 90% of adsorbed arsenic was recovered when arsenic-saturated BCF was treated with

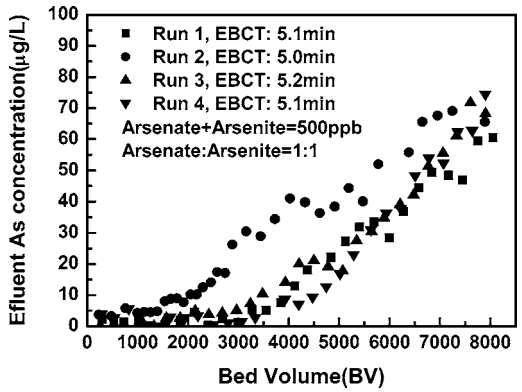

FIGURE 10. Performance of BCF in arsenic removal of the column test for four recycles (temperature 25 ± 0.5 °C, influent pH 7.0 ± 0.1, Fe content of BCF 220 mg/(mL of beads), influent As(III):As(V) = 250 μg/L:250 μg/L, EBCT = 5.0−5.2 min, SLV = 1.50−1.56 m/h).

TABLE 4. Concentrations of Background Ions from Influent and Effluent Solution[a]

	pH[b]	CO_3^{2-} (HCO_3^-)	SO_4^{2-}	PO_4^{3-}	SiO_3^{2-}	Ca^{2+}	Mg^{2+}	total Fe
influent	7.0	345	15.2	ND	10.1	66.8	40.5	0.03
effluent	7.4	346	15.5	ND	9.2	67.5	39.8	0.03

[a] Units of milligrams per liter. [b] No units.

strongly alkaline solutions. The regeneration process could be described as follows:

$$\equiv Fe-As(III,V) + OH^- \leftrightarrows Fe-OH + As(III,V)\ (K_{des})$$

As seen from Figure 10, high removal performance for arsenic was sustained in the four cycles. Breakthrough empty-bed volumes of four cycles at the WHO provisional guideline value of 10 μg/L for arsenic in drinking water were 3800, 2000, 3500, and 4400, respectively. The small breakthrough empty-bed volume in the second cycle (2000) in comparison with the other three cycles (3500−4400) could probably be attributed to the air bubbles produced during an intermittence of the column experiment resulting from the unpredictable power cut. Breakthroughs (50 μg/L) for four cycles were observed at 6800, 5700, 6700, and 6500 BV, respectively, after about 22 days of flowing through the fixed column for each cycle.

Induced by fractional dissolution of aluminia after regeneration, the removal performance of arsenic was only 75% of the virgin run. The other disadvantage of activated alumina regeneration was both sodium hydroxide and sulfuric acid should be used in the regeneration process (*10*, *19*). In contrast with the loss of activated alumina during the alkaline and acidic treatment, akaganéite was chemically stable through the regeneration. Due to the detachment of iron from the sand particles that escape along with the effluent during backwashing operations, 80−87% bed volumes were observed in the subsequent cycles for iron-coated sand (*25*, *55*). Compared with sands on which the iron oxides were exteriorly coated, resulting in desquamation, akaganéite was stably and uniformly impregnated into the interior pores of the cellulose. As seen in Table 4, the iron concentrations from influent and effluent solutions were both 0.03 mg/L, which was below WHO's iron MCL and showed no release of iron in the column runs. The examination of the iron amount in BCF indicated that no loss of Fe was found during the regeneration and column experiments too. XRD analysis illustrated that the Fe mineral phase was present as akaganéite crystals after four recycles and several months of immersion in alkaline solution. The stability of impregnated akaganéite, which was an important factor in sustaining the high removal efficiency of arsenic in the recycles, distinguished BCF from other adsorbents which were disturbed by the release of iron after regeneration. On the other side, BCF was retained in spherical geometry after four cycles and no bead crashes were found under the microscope. During long column runs and use of the same materials for four cycles, there was no significant increase in pressure drop. This indicated BCF is durably suited for fixed-bed column operation. Compared with precipitation and coagulation, the adsorption method does not need disposal of a large amount of iron sludge contaminated with arsenic. The concentrated arsenic in the regenerant solution can be further treated with cement and converted to a stabilized product which would not release arsenic into the environment.

To pursue the water quality of groundwater and examine the variations of dissolved ions after the column elution, the influent and effluent background ions were detected after 48 h of column experiments in the first cycle. As mentioned above, coexisting anions (e.g., sulfate, silicate, carbonate (bicarbonate), phosphate) are usually present in groundwater streams, possibly inhibiting arsenic removal. Therefore, these anions were detected, and the concentrations are listed in Table 4. It can be seen that the feedwater has high alkalinity with common concentrations of sulfate and silicate. The phosphate concentration is under the detection limit of ion chromatography. As seen from Table 4, the column runs did not have significant effects on the concentration of the major cations and anions such as Ca^{2+}, Mg^{2+}, and Fe^{3+}(Fe^{2+}) and CO_3^{2-} (HCO_3^-), SO_4^{2-}, and SiO_3^{2-}. This indicated that arsenic species were selectively adsorbed by BCF when interfering ions were present in the influent. On second thought, the effects of coexisting ions on column runs by BCF should be limited, considering unsymmetrical competition for adsorption sites between arsenic species and coexisting ions. However, the removal performance of arsenic by iron oxide-coated polymeric materials was significantly affected by the presence of other anions (*38*). As for cations such as Ca^{2+} in the groundwater, they were reported to cooperatively improve the removal performance of arsenic by hydrous ferric oxide (*21*). Besides inorganic competitive ions, organic substances (e.g., humic substances) are usually present in groundwater. However, when pH was equal to or higher than 7, it was found that humic substances had little effect on the arsenic removal efficiency (*21*). Therefore, it is considered that humic substances are not the major competitive anions for the removal of arsenic. Similar to that of the column run for arsenate, the effluent pH increased by 0.4 unit too. The increase of effluent pH was attributed to 250 μg/L arsenate present in the feedwater.

Preparation of BCF is cost effective for the following reasons: (i) the raw material and chemical agents are common and cheap and have a variety of sources (e.g., cotton cellulose, sodium hydroxide, carbon dioxide, and ferric chloride); (ii) the preparation procedures are simple, considering the loading process is realized through one step without functional steps (e.g., sulfuration) on cellulose, and energy-wasting manipulations such as extremely thermal treatments are seldom applied; (iii) some agents and materials can be recycled such as chloroben-pump oil used for shaping cellulose beads and fractional sodium hydroxide. It is concluded that BCF combines several advantages: (i) BCF is compatible with fixed-bed column processes with excellent mechanical strength and attrition resistance properties; (ii) BCF is selective toward both As(III) and As(V) species, showing high adsorption capacity in adsorption isotherms and large breakthrough bed volumes in column runs; (iii) the operations using BCF are very simple considering no pre- or posttreatment such as pH adjustment and oxidation treat-

ment were needed; (iv) BCF does not change water quality besides arsenic removal; (v) BCF shows high regeneration efficiency and high removal performance for arsenic, which were sustained in recycles. In conclusion, there are good prospects for BCF in practical applications for the removal of arsenic from contaminated groundwater.

Acknowledgments

This work was supported by the United Foundation of Nankai University and TianJin University, China. We thank Prof. Qiaoyun Huang, Faculty of Resources & Environment, Huazhong Agricultural University, China, and Dr. Le Zeng, Alberta Research Council Inc., Canada, for their warmhearted help and advice in revising this paper. Comments from anonymous reviewers significantly improved the manuscript too.

Literature Cited

(1) *1*) EPA. Arsenic in drinking water: health effects research. www.epa.gov/OGWDW/ars/ars10. html, 1999.
(2) WHO. Toxic effects of arsenic in humans. www.who.int/peh-super/Oth.lec/Arsenic/series4/002. htm, 1999.
(3) Smedley, P. L.; Kinniburgh, D. G. A review of the source, behaviour and distribution of arsenic in natural waters. *Appl. Geochem*. **2002**, *17*, 517−568.
(4) Chen, C. J.; Chiou, H. Y.; Huang, W. I.; Chen, S. Y.; Hsueh, Y. M.; Tseng, C. H.; Lin, L. J.; Shyu, M. P.; Lai, M. S. Systemic non-carcinogenic effects and developmental toxicity of inorganic arsenic. In *Arsenic Exposure and Health Effects*; Abernathy, C. O., Calderon, R. L., Chappell, W. R., Eds.; Chapman & Hall: London, 1997; p 124.
(5) Rudel, R.; Slayton, T. M.; Beck, B. D. Implications of arsenic genotoxicity for dose response of carcinogenic effects. *Regul. Toxicol. Pharm*. **1996**, *23*, 87−105.
(6) Schnoor, J. L., Ed. *Environmental Modeling: Fate and Transport of Pollutants in Water, Air, and Soil*; John Wiley & Sons: New York, 1996.
(7) Hering, J. G.; Chen, P.-Y.; Wilkie, J. A.; Elimelech, M. Arsenic removal from from drinking water by coagulation. *J. Environ. Eng*. **1997**, *123*, 800−807.
(8) Meng, X. G.; Korfiatis, G. P.; Bang, S.; Bang, K. W. Combined effects of anions on arsenic removal by iron hydroxides. *Toxicol. Lett*. **2002**, *133*, 103−111.
(9) Vagliasindi, F. G. A.; Benjamin, M. M. Arsenic removal in fresh and nom-preloaded ion exchange packed bed adsorption reactors. *Water Sci. Technol*. **1998**, *38* (6), 337−343.
(10) Singh, T. S.; Pant, K. K. Equilibrium, kinetics and thermodynamic studies for adsorption of As(III) on activated alumina. *Sep. Purif. Technol*. **2004**, *36*, 139−147.
(11) Pattanayak, J.; Mondal, K.; Mathew, S.; Lalvani, S. B. A parametric evaluation of the removal of As(V) and As(III) by carbon-based adsorbents. *Carbon* **2000**, *38*, 589−596.
(12) Raven, K. P.; Jain, A.; Loeppert, R. H. Arsenite and arsenate adsorption on ferrihydrite: kinetics, equilibrium, and adsorption envelopes. *Environ. Sci. Technol*. **1998**, *32*, 344−349.
(13) Driehaus, W.; Jekel, M.; Hiildebrandt, U. Granular ferric hydroxide- a new adsorbent for the removal of arsenic from natural water. *J. Water SRT Aqua* **1998**, *47*, 30−35.
(14) Muñoz, J. A.; Gonzalo, A.; Valiente, M. Arsenic adsorption by Fe(III)-loaded open-celled cellulose sponge. Thermodynamic and selectivity aspects. *Environ. Sci. Technol*. **2002**, *36*, 3405∼3411.
(15) Manning, B. A.; Goldberg, S. Adsorption and stability of arsenic-(III) at the clay mineral-water interface. *Environ. Sci. Technol*. **1997**, *31*, 1, 2005−2011.
(16) Fendorf, S.; Eick, M. J.; Grossl, P.; Sparks, D. L. Arsenate and chromate retention mechanisms on goethite. 1. surface structure. *Environ. Sci. Technol*. **1997**, *31*, 315−320.
(17) Lo, S. L.; Jeng, T. H.; Chin, L. H. Characteristics and adsorption properties of an iron coated sand. *Water Sci. Technol*. **1997**, *35*, 63−70.
(18) Lenoble, V.; Bouras, O.; Deluchat, V.; Serpaud, B.; Bollinger, J. C. Arsenic adsorption onto pillared clays and iron oxides. *J. Colloid Interface Sci*. **2002**, *255*, 52−58
(19) Lin, T.-F.; Wu, J.-K. Adsorption of arsenite and arsenate within activated alumina grains: equilibrium and kinetics. *Water Res*. **2001**, *35* (8), 2049−2057.
(20) Vaughan, R. L. J.; Reedb, B. E. Modeling As(V) removal by a iron oxide impregnated activated carbon using the surface complexation approach. *Water Res*. **2005**, *39*, 1005−1014.
(21) Wilkie, J. A.; Hering, J. G. Adsorption of arsenic onto hydrous ferric oxide: effects of adsorbate/adsorbent ratios and co-occurring solutes. *Colloids Surf., A* **1996**, *107*, 97−110.
(22) Lackovic, J. A.; Nikolaidis, N. P.; Dobbs, G. M. Inorganic arsenic removal by zero-valent iron. *Environ. Eng. Sci*. **2000**, *17* (1), 29−39.
(23) Su, C. M.; Puls, R. W. Arsenate and arsenite removal by zerovalent iron: kinetics redox transforation and implications for in situ groundwater remediation. *Environ. Sci. Technol*. **2001**, *35*, 1487−1492.
(24) Waypa, J. J.; Elimelech, M.; Hering, J. G. Arsenic removal by RO and NF membranes. *J.—Am. Water Works Assoc*. **1997**, *89* (10), 102−116.
(25) Benjamin, M. M.; Sletten, R. S.; Bailey, R. P.; Bennet, T. Sorption and filtration of metals using iron-oxide coated sand. *Water Res*. **1996**, *30*, 175−182.
(26) Bonnin, D.; Tampa, F. Method of removal arsenic species from an aqueous medium using modified zeolite minerals. U.S. Patent 006042731A, 2000.
(27) Ouvrard, S.; Simonnot, M. O.; Sardin, M. Reactive behavior of natural manganese oxides toward the adsorption of phosphate and arsenate. *Ind. Eng. Chem. Res*. **2002**, *41*, 2785−2791.
(28) Ouvrard, S.; Simonnot, M. O.; Donato, P.; Sardin, M. Diffusion-controlled adsorption of arsenate on a natural manganese oxide. *Ind. Eng. Chem. Res*. **2002**, *41*, 6194−6199.
(29) Fuhrman, H. G.; Tjell. J. C.; Mcconchie, D. Adsorption of arsenic from water using activated neutralized red mud. *Environ. Sci. Technol*. **2004**, *38*, 2428−2434.
(30) Tokunaga, S.; Wasay, S. A.; Park, S. W. Removal of arsenic(V) ion from aqueous solutions by lanthanum compounds. *Water Sci. Technol*. **1997**, *35*(7), 71−78.
(31) Suzuki, T. S.; Bomani, J. O.; Matsunaga, H.; Yokoyama, T. Preparation of porous resin loaded with crystalline hydrous zirconium oxide and its application to the removal of arsenic. *React. Funct. Polym*. **2000**, *43*, 165−172.
(32) Appelo, C. A. J.; Weiden, V. D.; Tournassat, C.; Charlet, L. Surface complexation of ferrous iron and carbonate on ferrihydrite and the mobilization of arsenic. *Environ. Sci. Technol*. **2002**, *36*, 3096−3103.
(33) Jain, A.; Raven, K. P.; Loeppert, R. H.Arsenite and arsenate adsorption on ferrihydrite: surface charge reduction and net OH^- release stoichiometry. *Environ. Sci. Technol*. **1999**, *33*, 1179−1184.
(34) Loukidoua, M. X.; Matisa, K. A.; Zouboulisa, A. I.; Kyriakidou, M. L. Removal of As(V) from wastewaters by chemically modified fungal biomass. *Water Res*. **2003**, *37*, 4544−4552.
(35) Huang, J. W.; Poynton, C. Y.; Kochian, L. V.; Elless, M. P. Phytofiltration of arsenic from drinking water using arsenic-hyper accumulating ferns. *J. Am. Chem. Soc.*, in press.
(36) DeMarco, M. J.; SenGupta, A. K.; Greenleaf, J. E. Arsenic removal using a polymeric/inorganic hybrid sorbent. *Water Res*. **2003**, *37*, 164−176.
(37) Matsunaga, H.; Yokoyama, T.; Eldridge, R. J.; Bolto, B. A. Adsorption characteristics of arsenic(III) and arsenic(V) on iron-(III)-loaded chelating resin having lysine-N^{α},N^{α}-diacetic acid moiety. *React. Funct. Polym*. **1996**, *29*, 167−174.
(38) Katsoyiannis, I. A.; Zouboulis, A I. Reoval of arsenic from contaminated water by sorption onto iron-oxide-coated polymeric materials. *Water Res*. **2002**, *36*, 5141−5155.
(39) Zeng, L. A method for preparing silica-containing iron(III) oxide adsorbents for arsenic removal. *Water Res*. **2003**, *37*, 4351−4358.
(40) Jang, M.; Shin, E. W.; Park, J. K.; Choi, S. I. Mechanisms of arsenate adsorption by highly-ordered nano-structured silicate media impregnated with metal oxides. *Environ. Sci. Technol*. **2003**, *37*, 5062−5070.
(41) Ahmed, M. F. Bangladesh University of Engineering and Technology (BUET), Dhaka, Bangladesh, 2001.
(42) Chwirka, J. D.; Thomson, B. M.; Stomp, J. M. Removing arsenic from groundwater. *J.*—Am. Water Works Assoc. **2000**, *92* (3), 79−88.
(43) Elizalde-González M. P.; Mattusch, J.; Einicke, W. D.; Wennrich, R.Sorption on natural solids for arsenic removal. *J. Chem. Eng*. **2001**, *81*, 187−195.
(44) Safiullah, S. *Proceedings of the International Conference on Arsenic in Bangladesh*, Dhaka, 1998; pp 8−12.

(45) Hering, J. G.; Chiu, Q. Arsenic occurrence and speciation in municipal ground-water-based supply system. *J. Environ. Eng. (Reston, Va.)* **2000**, *126* (5), 471−474.
(46) Driehaus, W.; Seith, R.; Jekel, M. Oxidation of arsenic(III) with manganese oxides in water treatment. *Water Res.* **1995**, *29* (1), 297−305.
(47) Bajpai, S.; Chaudhury, M. Removal of arsenic from manganese dioxide coated sand. *J. Environ. Eng. (Reston, Va.)* **1999**, *125* (8), 782−784.
(48) Frank, P.; Clifford, D. *As(III) oxidation and removal from drinking water*; EPA Project Summary, Report No. EPA/600/S2-86/021; Water Engineering Research Laboratory, Environment Protection Agency, Office of Research and Development: Cincinnati, OH, 1986.
(49) Kim, Y.; Kim, C.; Choi, I.; Rengaraj, S.; Yi, J. Arsenic removal using mesoporous alumina prepared via a templating method. *Environ. Sci. Technol.* **2004**, *38*, 924−931.
(50) Stamberg, J.; Peska, J. Preparation of porous spherical cellulose. *React. Polym.* **1983**, *1*, 145−147.
(51) Boeden, H. F.; Pommerening, K.; Becker, M.; Rupprich, C.; Holtzhauer, M. Bead cellulose derivatives as supports for immobilization and chromatographic purification and proteins. *J. Chromatogr.* **1991**, *552*, 389−414.
(52) Wolf, B. Bead cellulose products with film formers and solubilizers for controlled drug release. *Int. J. Pharm.* **1997**, *156*, 97−107.
(53) SEPAC (State Environmental Protection Administration of China). *Method of Detection and Analysis from Water and Wastewater*; China Environmental Science Press: Beijing, 2002; pp 308−311.
(54) Deliyanni, E. A.; Bakoyannakis, D. N.; Zouboulis, A. I.; Matis, K. A. Sorption of As(V) ions by akaganéite- type nanocrystals. *Chemosphere* **2003,** *50*, 155−163.
(55) Thirunavukkarasu, Q. S.; Viraraghavan, T.; Subramanian, K. S. Arsenic removal from drinking water using ion oxide-coated sand. *Water, Air, Soil Pollut.* **2003**, *142*, 95−111.
(56) Rajakoviv, L. V. The sorption of arsenic onto activated carbon impregnated with metallic silver and copper. *Sep. Sci. Technol.* **1992**, *27*, 1423.
(57) Jiang, J. Q. Removing arsenic from groundwater for the developing world—a review. *Water Sci. Technol.* **2001**, *44* (6), 89−98.
(58) Waychunas, G. A.; Davis, J. A.; Fuller, C. C. Geometry of sorbed arsenate on ferrihydrite and crystalline FeOOH: Re-evaluation of EXAFS results and topological factors in predicting sorbate geometry, and evidence for monodentate complexes. *Geochim. Cosmochim. Acta* **1995**, *59*, 3655−3661.
(59) Manceau, A. The mechanism of anion adsorption on iron oxides: Evidence for the bonding of arsenate tetrahedral on free Fe(O,OH)6 edges. *Geochim. Cosmochim. Acta.* **1995**, *59* (17), 3647−3653.
(60) Kwon, K. D.; Kubicki, J. D. Molecular orbital theory study on surface complex structures of phosphates to iron hydroxides: calculation of vibrational frequencies and adsorption energies. *Langmuir*, in press.
(61) Yamaguchi, N. U.; Okazaki, M.; Hashitani, T. Volume changes due to SO_4^{2-}, SeO_4^{2-}, and $H_2PO_4^-$ adsorption on amorphous iron (III) hydroxide in an aqueous suspension. *J. Colloid Interface Sci.* **1999**, *209*, 386-391.
(62) BGS, DPHE. Arsenic contamination of groundwater in Bangladesh. In *British Geological Survey*; Technical Report, WC/00/19.4 Volumes; Kinniburgh, D. G., Smedley, P. L., Eds.; British Geological Survey: Keyworth, U.K., 2001.
(63) Chen, S. L.; Dzeng, S. R.; Yang, M. H.; Chlu, K. H.; Shieh, G. M.; Wal, C. M. Arsenic species in groundwaters of the Blackfoot disease areas. Taiwan. *Environ. Sci. Technol.* **1994**, *28*, 877−881.
(64) Jiang, Z. X.; Zhan, J. Q.; Song, Z. X. *Ion Exchanger Engineering*; Tianjin University Press: Tianjin, China, 1992; p 206.
(65) Joshi, A.; Chaudhuri, M. Removal of arsenic from ground water by iron oxide-coated sand. *J. Environ. Eng.* **1996**, *122*, 769−771.

Received for review December 6, 2004. Revised manuscript received June 6, 2005. Accepted June 14, 2005.

ES048080K